Inventory of the Supplementary Information

- Table S4: Sequences of Primers, CRISPR Targeting Regions, and Morpholino.

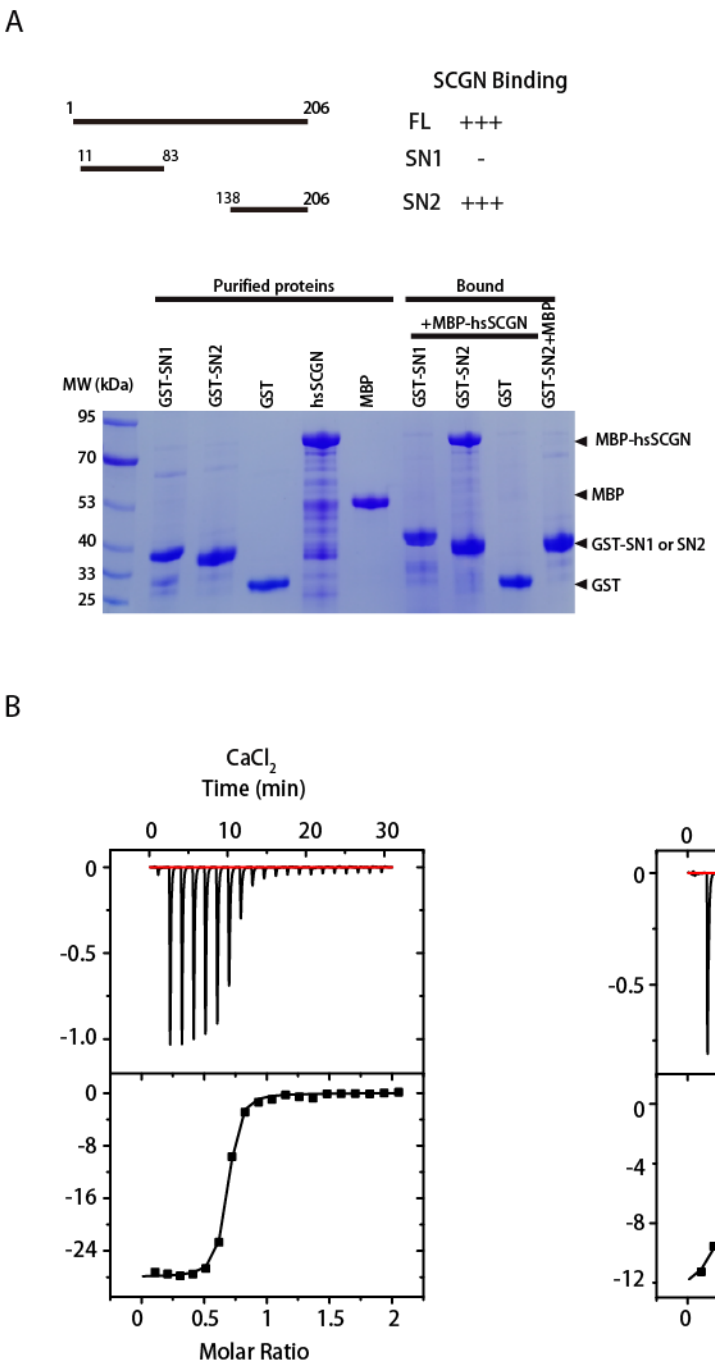

Fig. S1. Biochemical interaction bewteen SCGN and SNAP-25.

(A) GST pull-down assays performed with GST-SNAP-25 fragments or GST, and purified MBP-hsSCGN, in the presence of 2 mM $CaCl_2$ and 0.005% Triton X-100. After

incubation with soluble proteins, the resin was extensively washed. The resin-bound proteins were then subjected to SDS-PAGE and Coomassie Blue staining.

(B) Isothermal titration calorimetry of SNAP-25-J titrated into hsSCGN in a buffer containing 2 mM $CaCl_2$ (left) or 2 mM EDTA (right) at 25°C. Top and bottom panels show raw and integrated heat from injections, respectively. The black curve in the bottom panel represents a fit of the integrated data to a single-site binding model.

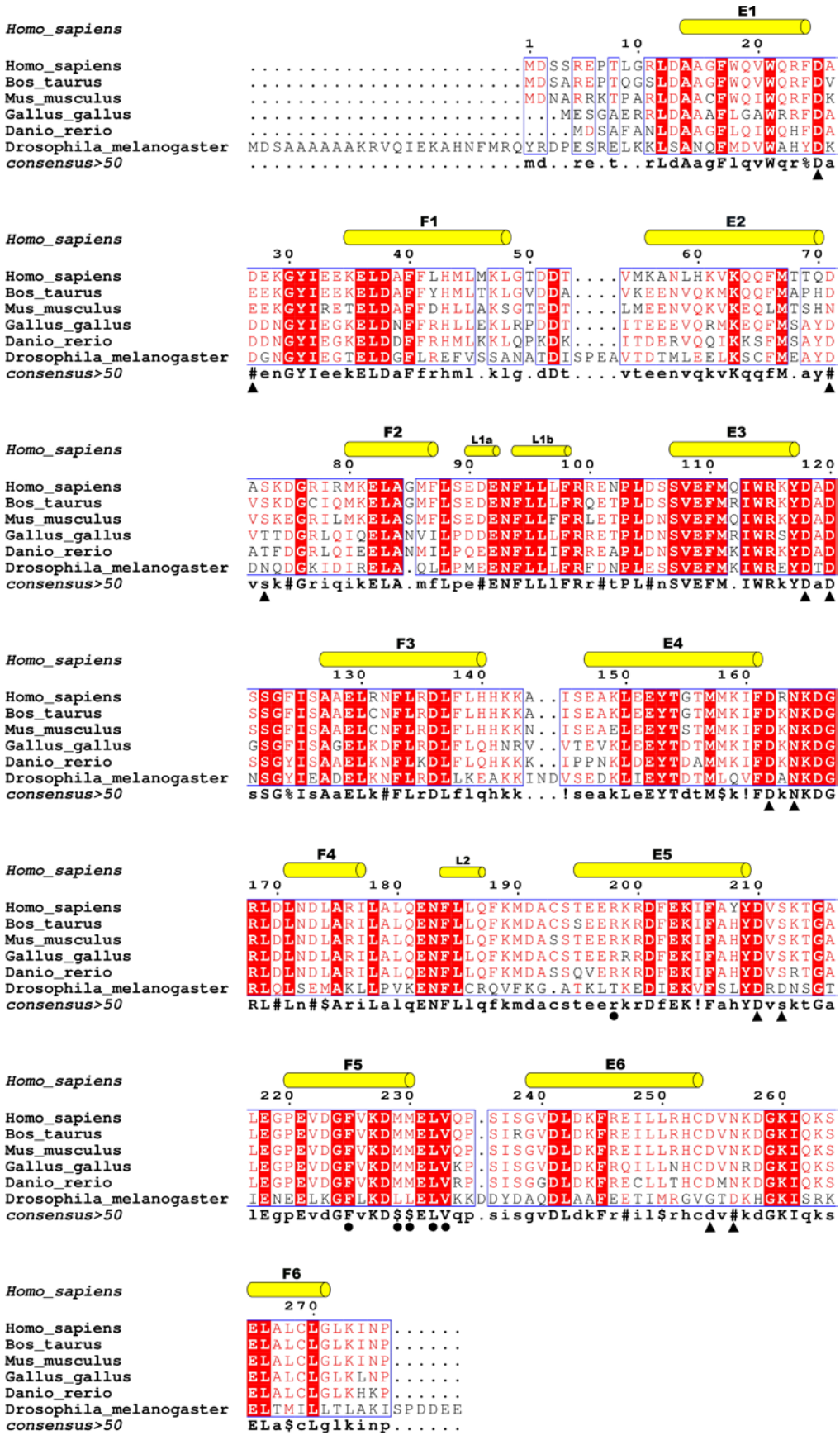
E1
Homo_sapiens
1 10 20
Homo_sapiens .....MDSSREPTLGRLDAAGFWQVWQRFDA
Bos_taurus .....MDSAREPTQGSLDAAGFWQVWQRFDV
Mus_musculus .....MDNARRKTPARLDAACFWQIWQRFDK
Gallus_gallus .....MESGAERRLDAAAFLGAWRRFDA
Danio_rerio .....MDSAFANLDAAGFLQIWQHFDA
Drosophila_melanogaster MDSAAAAAAKRVQIEKAHNFMRQYRDPESRELKKLSANQFMDVWAHYDK
consensus>50 .....md..re.t..rLdAagFlqvWqr%Da
F1
E2
Homo_sapiens
30 40 50 60 70
Homo_sapiens DEKGYIEEKELDAFFLHMLMKLGTDDT....VMKANLHKVKQQFMTTQD
Bos_taurus EEKGYIEEKELDAFFYHMLTKLGVDDA....VKEENVQKMKQQFMAPHD
Mus_musculus EEKGYIRETELDAFFDHLLAKSGTEDT....LMEENVQKVKEQLMTSHN
Gallus_gallus DDNGYIEGKELDNFFRHLLEKLRPDDT....ITEEEVQRMKEQFMSAYD
Danio_rerio DDNGYIEGKELDDFFRHMLKKLQPKDK....ITDERVQQIKKSFMSAYD
Drosophila_melanogaster DGNGYIEGTELDGFLREFVSSANATDISPEAVTDTMLEELKSCFMEAYD
consensus>50 #enGYIeekELDaFfrhml.klg.dDt....vteenvqkvKqqfM.ay#
F2
L1a
L1b
E3
Homo_sapiens
80 90 100 110 120
Homo_sapiens ASKDGRIRMKELAGMFLSEDENFLLLFRRENPLDSSVEFMQIWRKYDAD
Bos_taurus VSKDGCIQMKELAGMFLSEDENFLLLFRQETPLDSSVEFMRIWRKYDAD
Mus_musculus VSKEGRILMKELASMFLSEDENFLLFFRLETPLDNSVEFMQIWRKYDAD
Gallus_gallus VTTDGRLQIQELANVILPDDENFLLLFRRETPLDNSVEFMRIWRSYDAD
Danio_rerio ATFDGRLQIEELANMILPQEENFLLIFRREAPLDNSVEFMKIWRKYDAD
Drosophila_melanogaster DNQDGKIDIRELA.QLLPMEENFLLLFRFDNPLESSVEFMKIWREYDTD
consensus>50 vsk#GriqikELA.mfLpe#ENFLLlFRr#tPL#nSVEFM.IWRkYDaD
F3
E4
Homo_sapiens
130 140 150 160
Homo_sapiens SSGFISAAELRNFLRDLFLHHKKA..ISEAKLEEYTGTMMKIFDRNKDG
Bos_taurus SSGFISAAELCNFLRDLFLHHKKA..ISEAKLEEYTGTMMKIFDKNKDG
Mus_musculus SSGFISAAELCNFLRDLFLHHKKN..ISEAELEEYTSTMMKIFDKNKDG
Gallus_gallus GSGFISAGELKDFLRDLFLQHNRV..VTEVKLEEYTDTMMKIFDKNKDG
Danio_rerio SSGYISAAELKNFLKDLFLQHKKK..IPPNKLDEYTDAMMKIFDKNKDG
Drosophila_melanogaster NSGYIEADELKNFLRDLLKEAKKINDVSEDKLIEYTDTMLQVFDANKDG
consensus>50 sSG%IsAaELk#FLrDLflqhkk...!seakLeEYTdtM$k!FDkNKDG
F4
L2
E5
Homo_sapiens
170 180 190 200 210
Homo_sapiens RLDLNDLARILALQENFLLQFKMDACSTEERKRDFEKIFAYYDVSKTGA
Bos_taurus RLDLNDLARILALQENFLLQFKMDACSSEERKRDFEKIFAHYDVSKTGA
Mus_musculus RLDLNDLARILALQENFLLQFKMDASSTEERKRDFEKIFAHYDVSKTGA
Gallus_gallus RLDLNDLARILALQENFLLQFKMDACSTEERRRDFEKIFAHYDVSKTGA
Danio_rerio RLDLNDLARILALQENFLLQFKMDASSQVERKRDFEKIFAHYDVSRTGA
Drosophila_melanogaster RLQLSEMAKLLPVKENFLCRQVFKG.ATKLTKEDIEKVFSLYDRDNSGT
consensus>50 RL#Ln#$AriLalqENFLlqfkmdacsteerkrDfEK!FahYDvsktGa
F5
E6
Homo_sapiens
220 230 240 250 260
Homo_sapiens LEGPEVDGFVKDMMELVQP.SISGVDLDKFREILLRHCDVNKDGKIQKS
Bos_taurus LEGPEVDGFVKDMMELVQP.SIRGVDLDKFREILLRHCDVNKDGKIQKS
Mus_musculus LEGPEVDGFVKDMMELVQP.SISGVDLDKFREILLRHCDVNKDGKIQKS
Gallus_gallus LEGPEVDGFVKDMMELVKP.SISGVDLDKFRQILLNHCDVNRDGKIQKS
Danio_rerio LEGPEVDGFVKDMMELVRP.SISGGDLDKFRECLLTHCDMNKDGKIQKS
Drosophila_melanogaster IENEELKGFLKDLLELVKKDDYDAQDLAAFEETIMRGVGTDKHGKISRK
consensus>50 lEgpEvdGFvKD$$ELVqp.sisgvDLdkFr#il$rhcdv#kdGKIqks
F6
Homo_sapiens
270
Homo_sapiens ELALGLGLKINP......
Bos_taurus ELALGLGLKINP......
Mus_musculus ELALGLGLKINP......
Gallus_gallus ELALGLGLKLNP......
Danio_rerio ELALGLGLKHKP......
Drosophila_melanogaster ELTMILLTLAKISPDDEE
consensus>50 ELa$cLglkinp......

Fig. S2. Sequence comparision of SCGN from different model organisms.

Sequence alignments were performed with ClustalW, with protein secondary structure listed above and consensus sequence listed below. ●: SNAP-25-binding residues confirmed by biochemical studies; ▲: Calcium-binding residues mutated in this study.

A

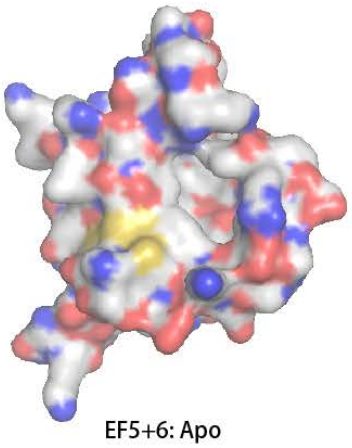

EF5+6: Apo

B

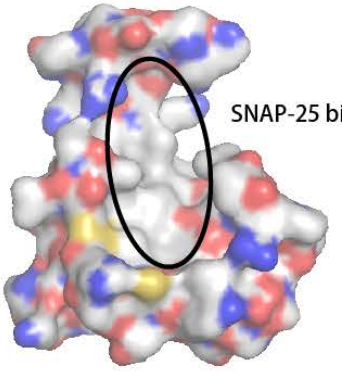

EF5+6: Holo

C

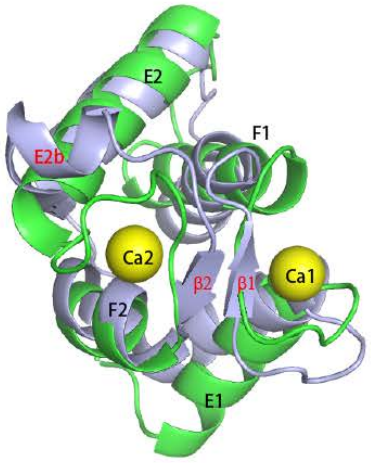

EF1+2

D

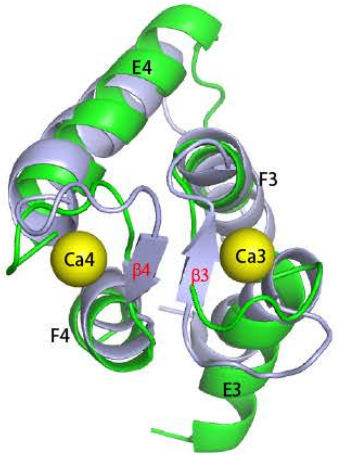

EF3+4

E

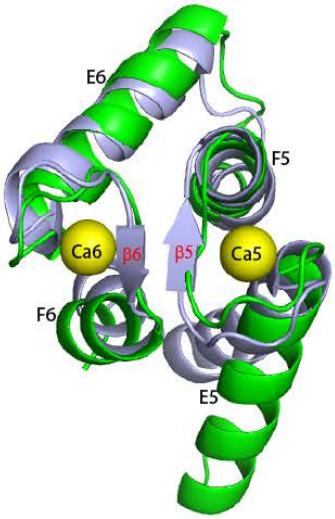

EF5+6

Fig. S3. Structural comparison of SCGN in the Apo and Holo forms.

(A-B) Surface presentation of EF hands 5+6 of SCGN in the Apo (A) and Holo forms (B). Oval indicating the SNAP-25 binding groove. Blue: N atoms; red: O atoms; silver: C atoms; yellow: S atoms.

(C-E) All EF hands of SCGN undergo significant conformational changes upon the binding to Ca^{2+} and SNAP-25. Structural overlay of EF hands 1+2 (C), 3+4 (D), and 5+6 (E), of SCGN in the Apo (light blue) and Holo forms (green). The unique secondary structures, including the two-stranded β-sheets and helice E2b, in the apo form, are labled in red.

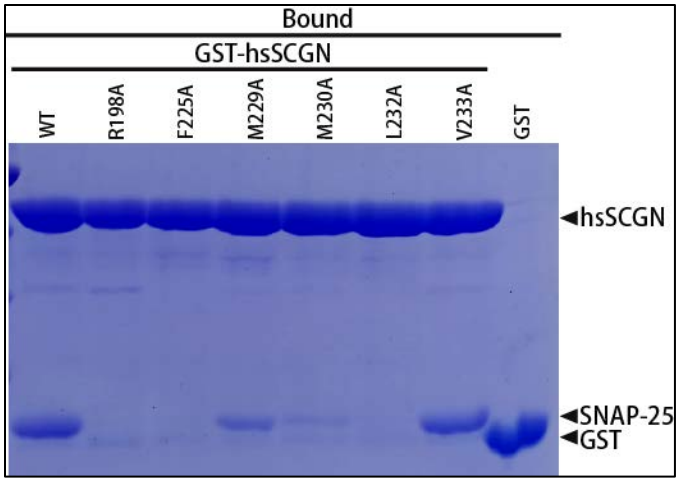

Fig. S4. GST-hsSCGN wild-type or mutants, or GST pull-down of SNAP-25.

GST pull-down assays performed with GST-hsSCGN wild-type or mutants, or GST, and purified SNAP-25 protein, in the presence of 2 mM $CaCl_2$ and 0.5% Triton X-100. After incubation with soluble proteins, the resin was extensively washed. The resin-bound proteins were then subjected to SDS-PAGE and Coomassie Blue staining.

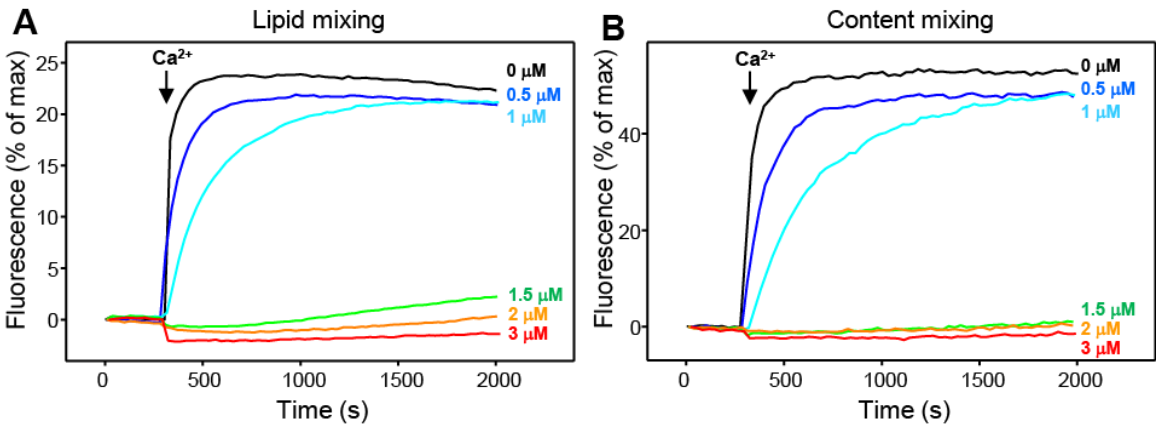

Fig. S5. SCGN inhibits SNARE-dependent liposome fusion through interactions with SNAP-25.

Lipid mixing (A) between V- and T-liposomes was monitored from the fluorescence de-quenching of Marina Blue lipids, and content mixing (B) was monitored from the increase in the fluorescence signal of Cy5-streptavidin trapped in the V-liposomes caused by FRET with PhycoE-biotin trapped in the T-liposomes upon liposome fusion. Assays were performed with V- and T-liposomes in the presence of Munc18-1, $M13C_1C_2BMUNC_2C$, NSF, SNAP and variable concentrations of SCGN as indicated by the color-coded labels. Experiments were started in the presence of 100 μM EGTA and 5 μM streptavidin, and Ca^{2+} (600 μM) was added at 300 s.

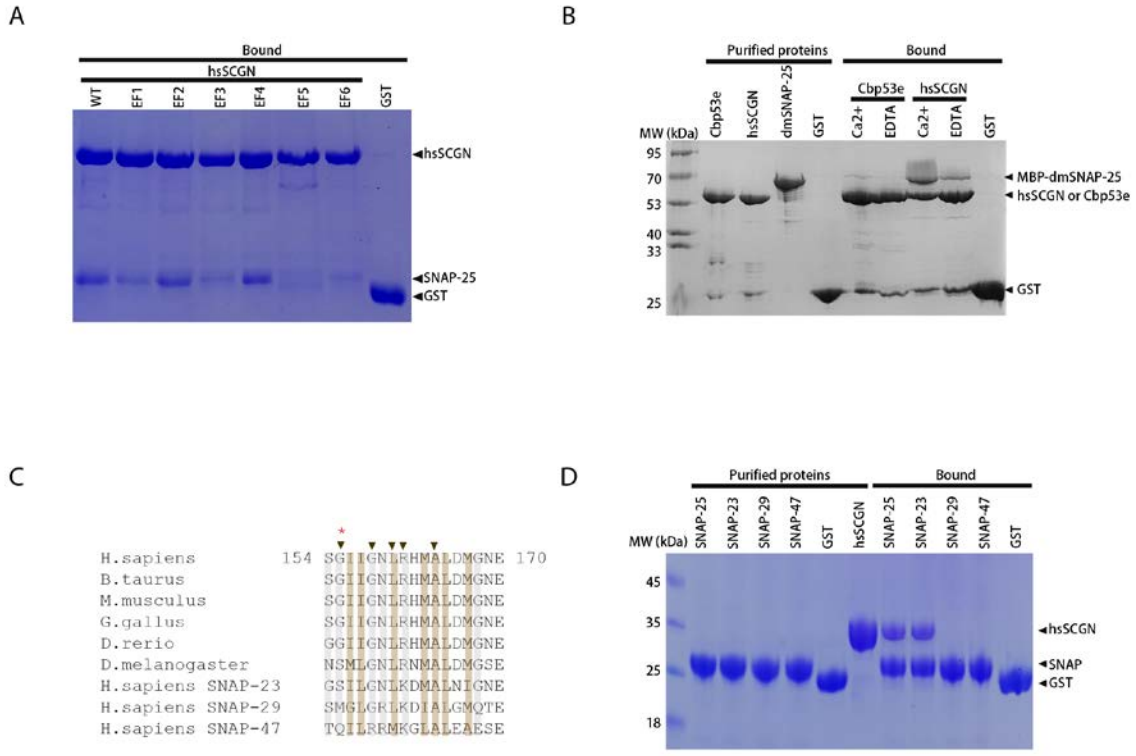

Fig. S6. Mutagensis to verify the interaction between SCGN and SNAP-25.

(A) GST pull-down assays performed with GST-hsSCGN wild-type or mutants, or GST, and purified SNAP-25 protein, in the presence of 2 mM $CaCl_2$ and 0.5% Triton X-100. After incubation with soluble proteins, the resin was extensively washed. The resin-bound proteins were then subjected to SDS-PAGE and Coomassie Blue staining. EF1, EF2, EF3, EF4, EF5, EF6: alanine subsitution of the 1st and 3rd positions of the loop in each EF.

(B) GST pull-down assays performed with GST-Cbp53e, hsSCGN, or GST, and purified MBP-*Drosophila*-SNAP-25 (dmSNAP-25), in the presence of 2 mM $CaCl_2$ and 0.005% Triton X-100. After incubation with soluble proteins, the resin was extensively washed.

Shown is a Coomassie blue–stained SDS–PAGE gel of purified proteins (left) and resin-bound samples (right).

(C) Sequence alignments of hsSNAP-25 (aa154-170) and its corresponding SNAP-25 sequences from representative organisms. The corresponding sequences from human SNAP-23, SNAP-29 and SNAP-47 are also listed. Residues contacting SCGN are highlighted either in grey (non-hydrophobic) or machaccino (hydrophobic residues). ▼: residues whose substitutions weaken the binding toward SCGN; *: residue mutated in the vesicle fusion assay.

(D) GST pull-down assays performed with GST-SNAP-25-J, or its corresponding residues in SNAP-23, SNAP-29, SNAP-47, or GST, and purified hsSCGN, in the presence of 2 mM $CaCl_2$ and 0.5% Triton X-100. After incubation with soluble protein(s), the resin was extensively washed. Shown is a Coomassie blue–stained SDS–PAGE gel of purified proteins (left) and resin-bound samples (right).

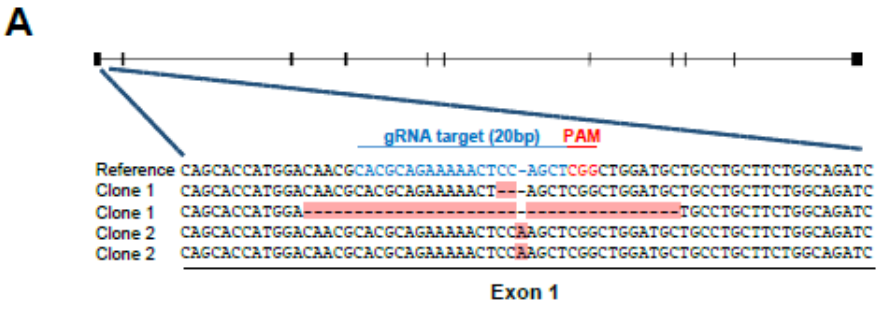

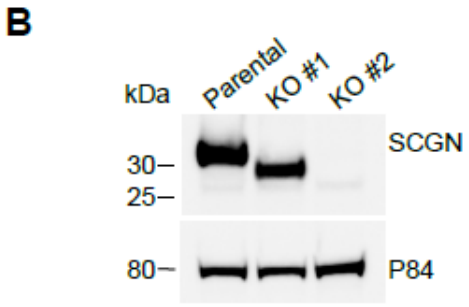

Fig. S7. Engineering *Scgn*-deficient STC-1 clones by CRISPR/Cas9 technology.

(A) Diagram depicting CRISPR/Cas9 targeting of exon 1 of mouse *Scgn*. Sequence of guide RNA is colored in blue, and PAM in red. Reference sequence (top), sequences of Clones 1 and 2 are shown. Note that clone 1 has at least 2 independent indel events.

(B) Expression level of SCGN in parental, KO #1, KO #2 STC-1 cells, determined by immunoblotting.

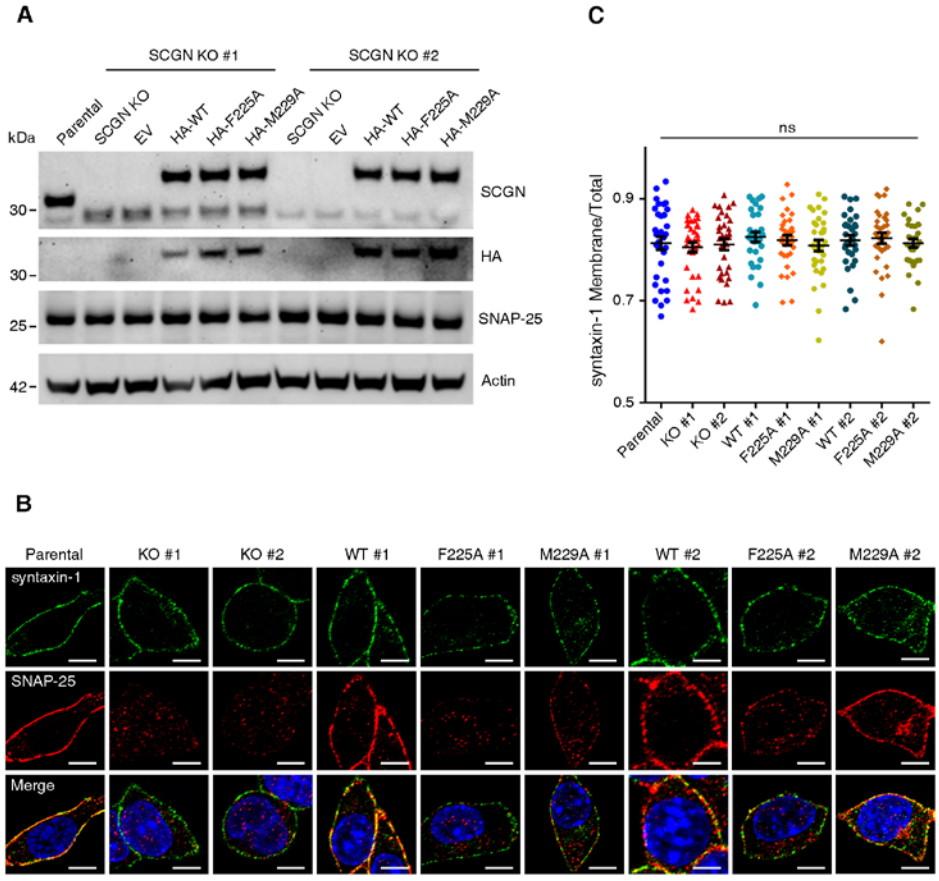
A
SCGN KO #1
SCGN KO #2
kDa
Parental
SCGN KO
EV
HA-WT
HA-F225A
HA-M229A
SCGN KO
EV
HA-WT
HA-F225A
HA-M229A
30
30
25
42
SCGN
HA
SNAP-25
Actin
C
ns
syntaxin-1 Membrane/Total
0.9
0.7
0.5
Parental
KO #1
KO #2
WT #1
F225A #1
M229A #1
WT #2
F225A #2
M229A #2
B
Parental
KO #1
KO #2
WT #1
F225A #1
M229A #1
WT #2
F225A #2
M229A #2
syntaxin-1
SNAP-25
Merge

Fig. S8. SCGN does not control the subcellular localization of syntaxin-1.

(A) Protein levels in cell lysates of SCGN deficient and rescue STC-1 cells, determined by western blotting. SCGN deficent cell-lines were generated using the CRISPR/Cas9 technology. Two individual clones were chosen, and lentiviral reexpressed with N-terminal HA-tagged-SCGN (WT, F225A, M229A) or empty vector (EV).

(B) Parental, SCGN-KO clones and rescue STC-1 cells were co-stained with anti-syntaxin-1 and anti-SNAP-25 antibodies. Scale bars, 10μm.

(C) Quantification of syntaxin-1 levels in cells in (B). Membranous and total cellular fluorescence intensity ratio was calculated from 35 cells on average in each group. Bars, mean; error bars, SEM, differences among groups by unpaired student *t*-test. ns, not significant.

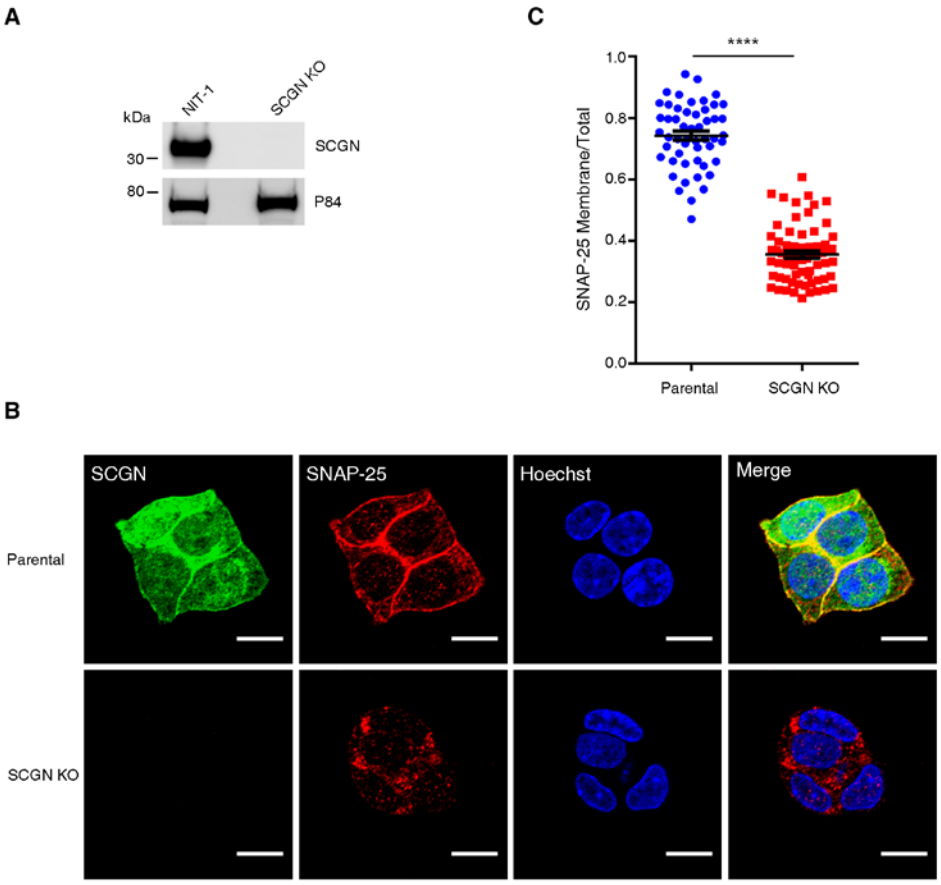
A
NIT-1
SCGN KO
kDa
30
80
SCGN
P84
C
****
SNAP-25 Membrane/Total
1.0
0.8
0.6
0.4
0.2
0.0
Parental
SCGN KO
B
SCGN
SNAP-25
Hoechst
Merge
Parental
SCGN KO

Fig. S9. SCGN promotes plasma membrane localization of SNAP-25 in pancreatic beta cells.

(A) Protein levels in cell lysates of parental and SCGN-KO NIT-1 cells, determined by immunoblotting. SCGN-KO cells were generated using the CRISPR/Cas9 technology, and clonal cell lines were isolated for this study.

(B) Parental and SCGN KO NIT-1 were co-stained with anti-SCGN and anti-SNAP-25 antibodies. Representative cells were shown. Scale bars, 10μm. Blue: DAPI staining.

(C) Quantification of SNAP-25 membranous and total cellular fluorescence intensity ratio was calculated from each cell lines used in (B). Over 50 cells were used for analysis in each group. Bars, mean; error bars, SEM, differences among groups by unpaired student *t*-test. ****, $P < 0.0001$.

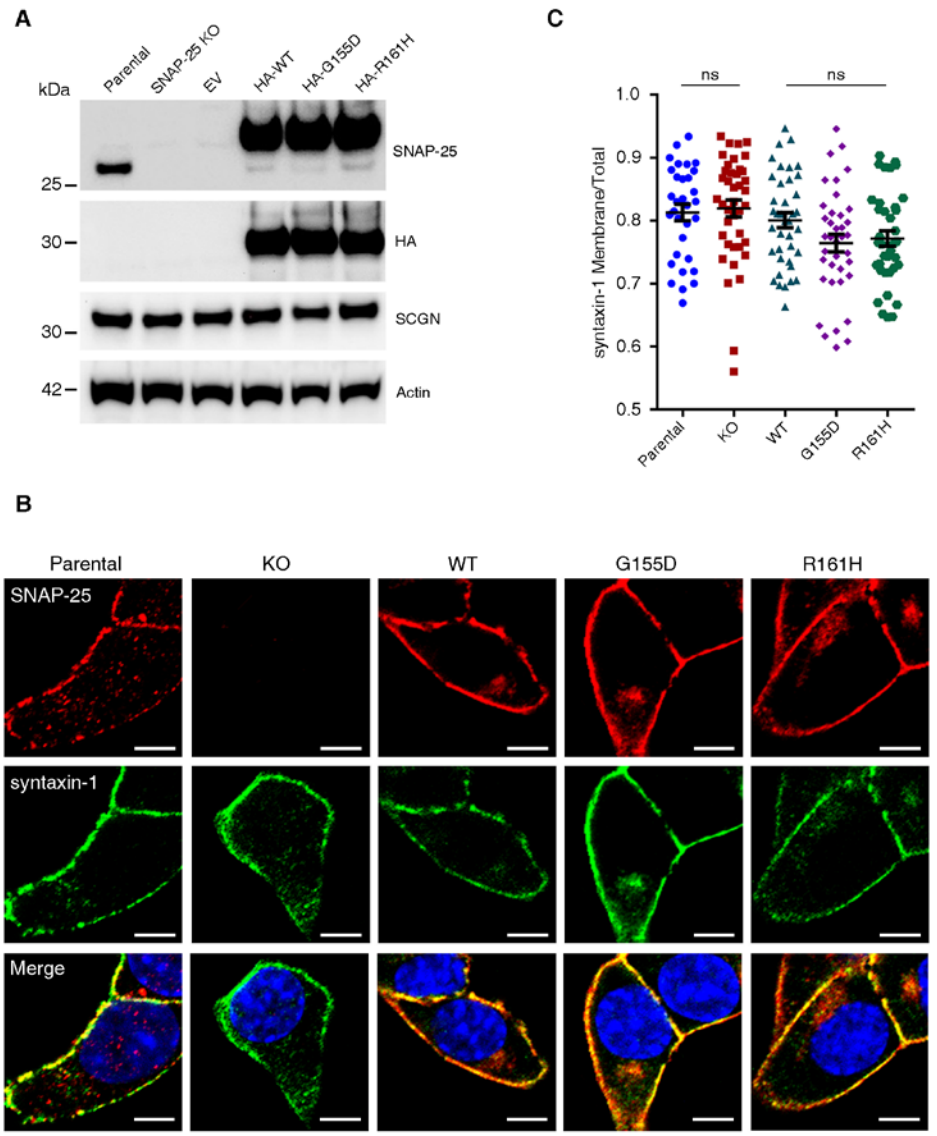
A
kDa
Parental
SNAP-25 KO
EV
HA-WT
HA-G155D
HA-R161H
SNAP-25
25
HA
30
SCGN
30
Actin
42
C
ns
ns
syntaxin-1 Membrane/Total
1.0
0.9
0.8
0.7
0.6
0.5
Parental
KO
WT
G155D
R161H
B
Parental
KO
WT
G155D
R161H
SNAP-25
syntaxin-1
Merge

Fig. S10. Knockout of SNAP-25 does not alter the subcellular localization of syntaxin-1.

(A) Protein levels in cell lysates of SNAP-25 deficient and rescue STC-1 cells, determined by western blotting. SNAP-25 deficent cell-lines were generated using the CRISPR/Cas9 technology. The KO clone was lentiviral reexpressed with N-terminal HA-tagged-SNAP25 (WT, G155D, R161H) or empty vector (EV).

(B) Parental, SNAP25-KO and SNAP25-KO rescue STC-1 cells were co-stained with anti-syntaxin-1 and anti-SNAP-25 antibodies. Scale bars, 10μm.

(C) Quantification of syntaxin-1 levels in cells in (B). Membranous and total cellular fluorescence intensity ratio was calculated from 38 cells on average in each group. Bars, mean; error bars, SEM, differences among groups by unpaired student *t*-test. ns, not significant.

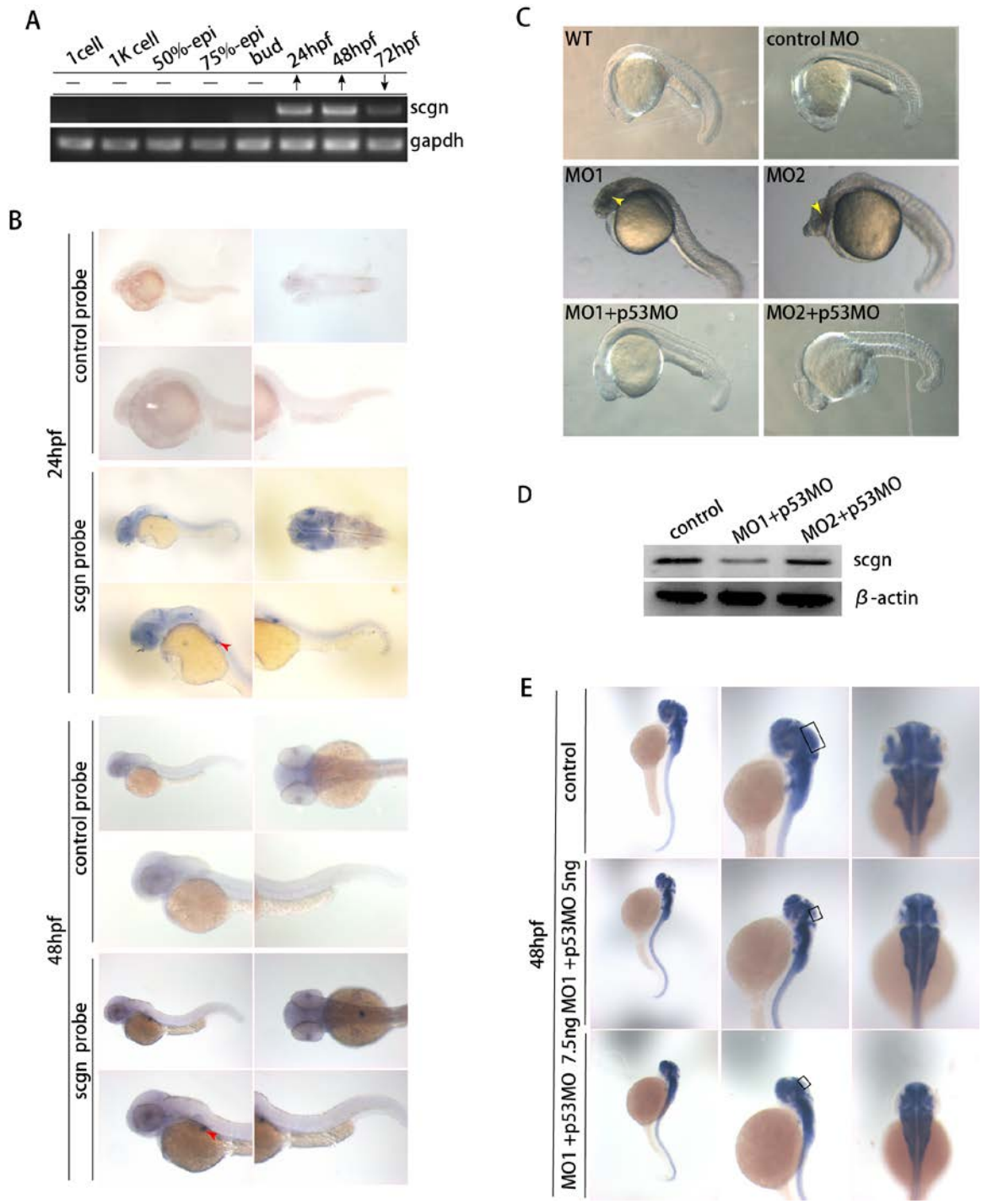

Fig. S11. Knockdown of SCGN leads to abnormal brain development in zebrafish.

(A) The mRNA expression levels of SCGN at the indicated developmental stages of zebrafish embryos are shown. GAPDH is used as reference. Epi, epiboly; bud, tail bud; hpf, hours post fertilization.

(B) Whole-mount in situ hybridization analysis of SCGN expression in zebrafish embyros at 24 and 48hpf. Red triangles indicate the pancreas.

(C) The injection of SCGN MO1 or MO2 led to the apoptosis of brain cells (indicated by the yellow arrow) at 24 hpf, which could be relieved by the co-injection of p53 MO WT:wild-type; control MO: control MO injection; MO1: MO1 injection; MO2: MO2 injection; MO1+p53 MO: MO1 and p53 MO co-injection; MO2+p53 MO: MO2 and p53 MO co-injection.

(D) Immunoblot of entire zebrafish tissue extracts showing that injection of MO1 or MO2 effectively decreased the protein level of SCGN. WT: wild-type; MO1+p53 MO: co-injection of MO1 and p53 MO; MO2+p53 MO: co-injection of MO1 and p53 MO. All injections were performed at one cell stage of zebrafish development. β-actin was used as a loading control. Injection of MO1 and MO2 suppressed 70% and 40% of the SCGN protein level, respectively.

(E) The severity of the zebrafish phenotype correlated with the amount of MO1 injected.At the 48 hpf stage, the size of zebrafish midbrain decreased with increasing amount of MO1. The black rectangles indicate the midbrain of zebrafish embryos. Left, lateral view of whole fish. Middle, lateral view of the brain. Right, top view of the brain.

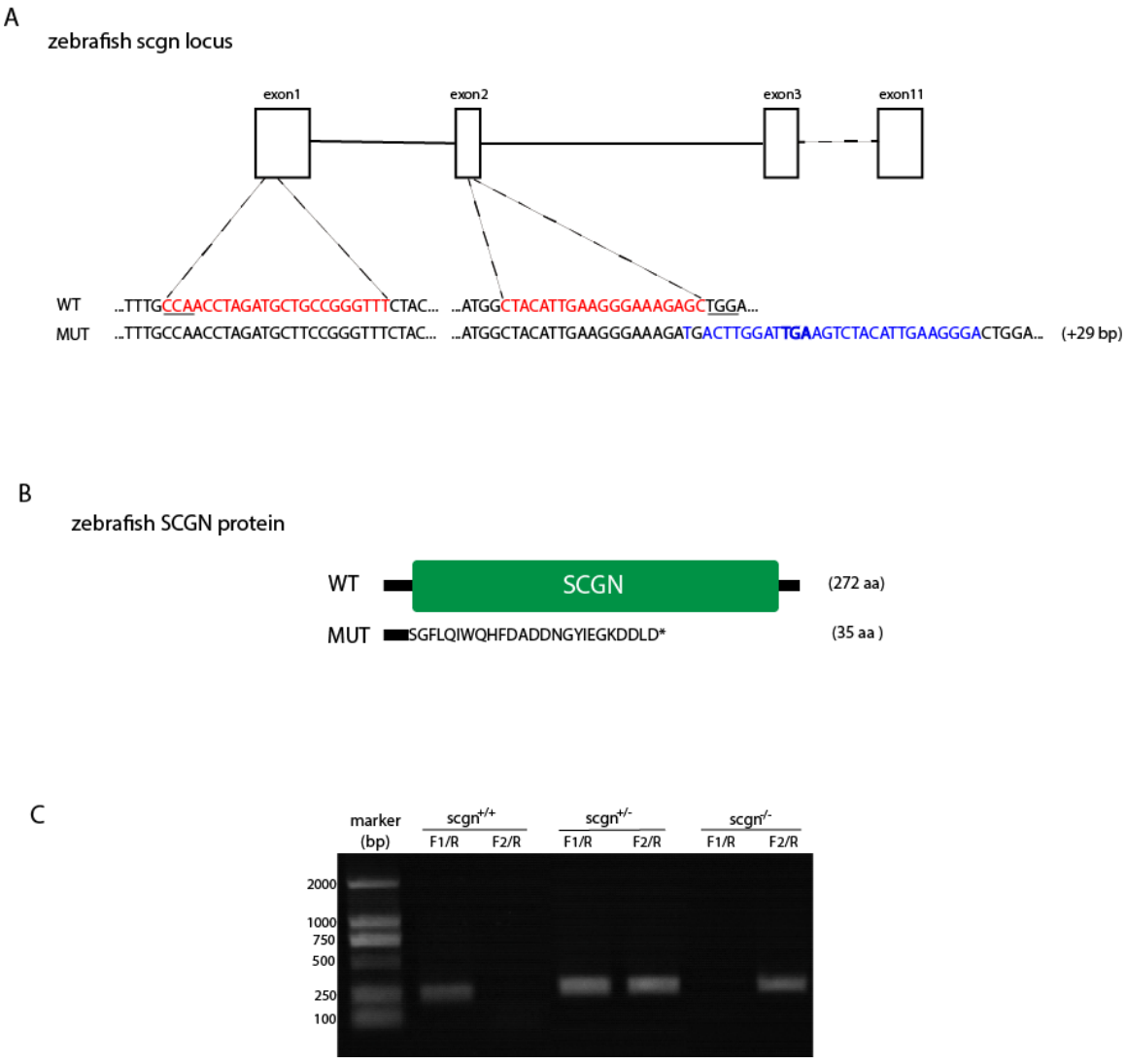

Fig. S12. SCGN knockout in zebrafish.

(A) CRISPR/Cas9-mediated SCGN knockout. Guide RNA targeting sequences are highlighted in red, and PAM is marked with an underscore. We recovered a stablytransmitted mutant allele, which carrys a single nucleotide mutation in exon 1 and 29 bp insertion within exon 2. The altered nucleotides are colored in blue.

(B) Protein sequences of SCGN WT and the truncated form encoding by the SCGN knockout zebrafish. The truncated proteins contain only 35 amino acids, due to an early termination of translation.

(C) Genotyping results of WT, SCGN heterozygouos, and homogous zebrafish. The primer sequences used for genotyping are given in Table S4.

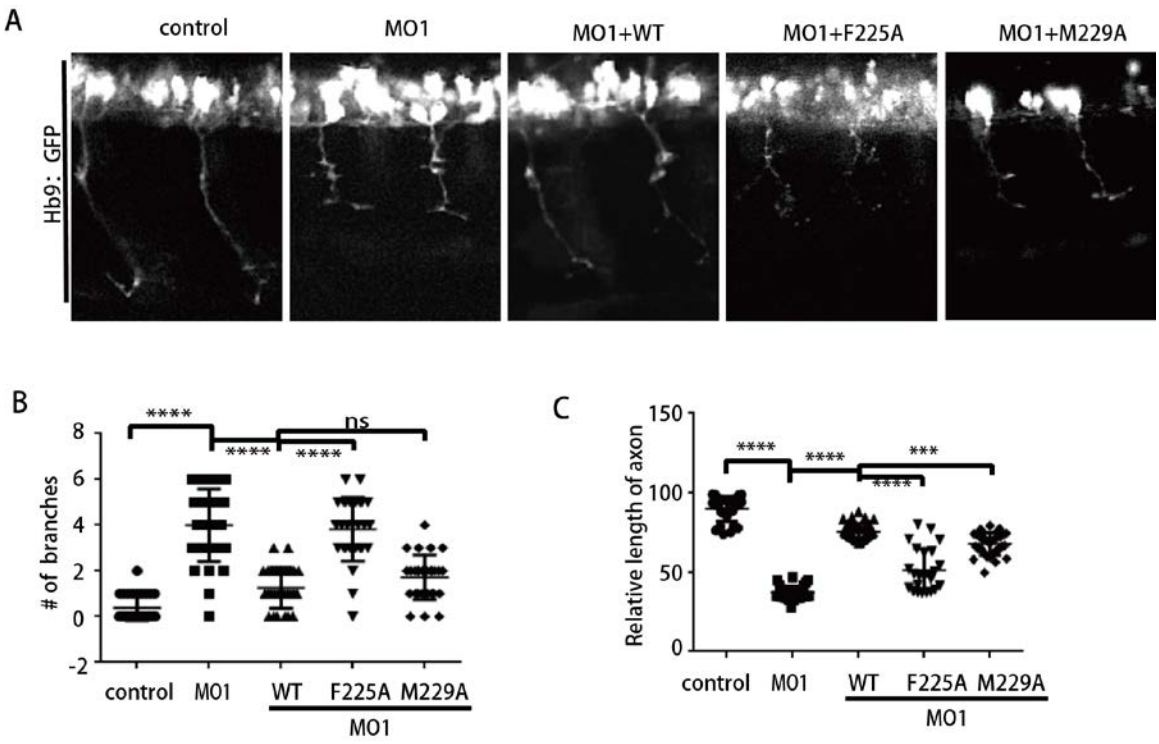

Fig. S13. SCGN is critical for normal development of motor neuron.

(A) Morphology of CaP axons from embryos at 48 hpf that were injected MO1 and/or different mRNA. All injections are performed at one cell stage of the Tg [hb9: GFP]^{ml2} transgenic zebrafish embryos.

(B) Statistical results of the branch number of CaP axons in embryos treated as in A. For each group, ~30 axons from severn to nine Tg [hb9: GFP]^{ml2} transgenic zebrafish embryos are scored. Experiments were repeated three times. Mean ±SD, ****P < 0.0001; ns, not significant. P values were calculated using one-way ANOVA, Tukey's multiple comparisons test.

(C) Statistical results of relative length of CaP axons in embryos treated as in A. For each group, ~30 axons from severn to nine Tg [hb9: GFP]^{ml2} transgenic zebrafish embryos are scored. Experiments were repeated three times. Mean ±SD, ****P < 0.0001; ***P <

0.001. P values were calculated using one-way ANOVA, Tukey's multiple comparisons test.

Fig. S14. Overexpression of SNAP-25 failed to to restore hormone secretion in STC-1 deficient cells.

(A) Expression of SNAP-25 in indicated cell lines, determined by immunoblotting.

(B) Immunofluorescence (IF) images of parental STC-1 cells, and SCGN KO #2 rescued with empty vector (EV) or HA-SNAP-25. Representative cells are shown. Images for red channel in parental and EV clones were obtained at 200% brightness level than that of HA-SNAP25 overexpressing cells. Scale bar, 16 μm.

(C) GLP-1 secretion assay. GLP-1 measured from indicated cell lines before or after fatty acid (DHA) stimulation. Error bars, S.E.M, unpaired student *t*-test was used. **** $P < 0.0001$.

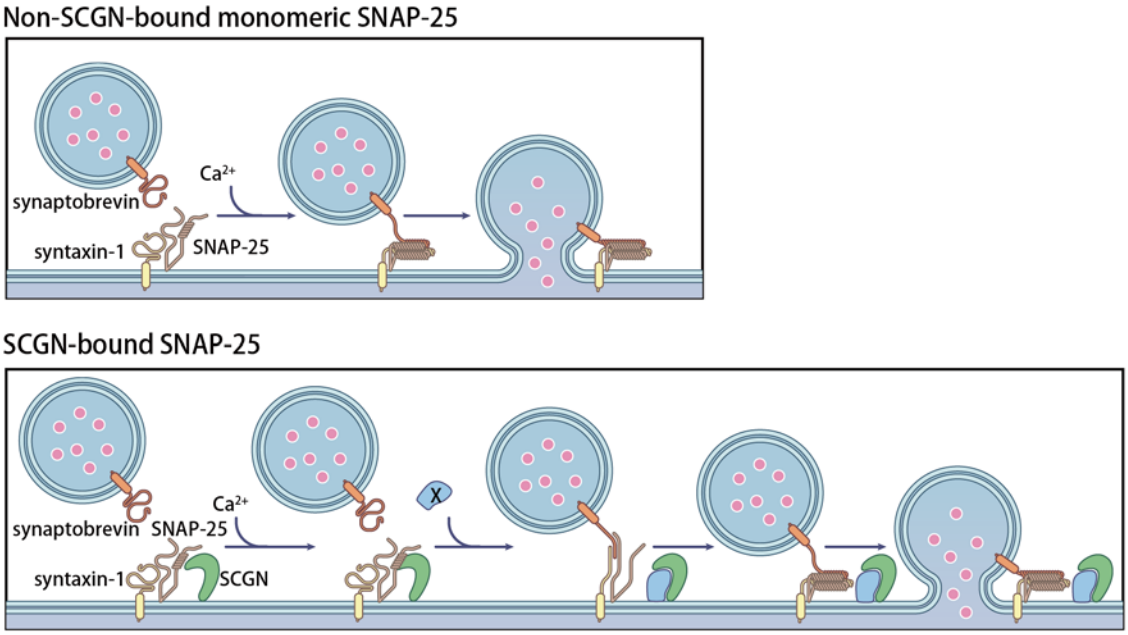

Fig. S15. A model showing how SCGN may regulate SNARE function and exocytosis.

SCGN interacts with the C-terminus of SNAP-25, and promotes its plasma membrane localization. On the plasma membrane, some SNAP-25 could associate with SCGN whereas some SNAP-25 does not. Top: Non-SCGN-bound monomeric SNAP-25 can quickly respond to calcium signals and form the SNARE complex to mediate vesicle exocytosis. Bottom: For the SCGN-bound SNAP-25, calcium influx dramatically enhances the interaction between SCGN and SNAP-25, inhibiting SNARE complex assembly. The inhibition needs to be released by an unknown protein or lipid (X), which displaces SNAP-25 from SCGN. Thus, SCGN could mediate slow modes of vesicle exocytosis. Other SNARE modulators, such as Munc-13, Munc-18 and synaptotagmin-1, are omitted for simplicity.

Table S1. Crystallography Data Collection and Refinement Statistics.

	SCGN-SNAP-25-Ca^{2+}
Cell axial lengths (Å)	a=104.5, b= 107.0, c= 54.7
Spacegroup	$P2_12_12$
Data collection	
Resolution range (Å)	50.00-2.37 (2.41-2.37)
Number of observed reflections	964901 (24390)
Number of unique reflections	25808 (1167)
Completeness (%)	99.6 (99.1)
Redundancy	37.4 (20.9)
R_{pim}	0.035 (0.342)
Highest shell CC1/2	0.639
Mean I/I_{sigma}	19.7 (1.3)
Refinement	
Resolution range (Å)	49.96-2.37 (2.43-2.37)
Number of working reflections	20354 (955)
Number of test reflections	1950 (89)
R_{work} [a] (no. of reflections)	0.200 (0.261)
R_{free} [b] (no. of reflections)	0.237 (0.308)
R.m.s. deviation bond lengths (Å)	0.009
R.m.s. deviation bond angles (°)	1.591
Mean B value	38.1
Ramachandran plot	
Most favored regions (%)	98.34
Allowed regions (%)	1.66
Disallowed regions (%)	0.0

R_{work} [a] = $\Sigma|Fo - Fc|/|Fo|$, where Fc and Fo are the calculated and observed structure factor amplitudes, respectively
R_{free} [b] calculated as for R_{work} but for 5.0% of the total reflections chosen at random and omitted from refinement for all data sets
values in the parenthesis is information from highest resolution shell.

Table S2. DNA Constructs Used in this Study.

Construct name	Description[#1]	Source or reference
ZebrafishsSCGN		
drSCGN	GST-Tev-drSCGN full length	(Bitto et al)
Human SCGN		
hsSCGN	GST-Tev-hsSCGN full length	This study
hsSCGN R198A	GST-Tev-hsSCGN full length R198A	This study
hsSCGN F225A	GST-Tev-hsSCGN full length F225A	This study
hsSCGN M229A	GST-Tev-hsSCGN full length M229A	This study
hsSCGN L230A	GST-Tev-hsSCGN full length L230A	This study
hsSCGN L232A	GST-Tev-hsSCGN full length L232A	This study
hsSCGN V233A	GST-Tev-hsSCGN full length V233A	This study
hsSCGN D25A/D27A	GST-Tev-hsSCGN full length D25A/D27A	This study
hsSCGN D71A/S73A	GST-Tev-hsSCGN full length D71A/S73A	This study
hsSCGN D118A/D120A	GST-Tev-hsSCGN full length D118A/D120A	This study
hsSCGN D161A/N163A	GST-Tev-hsSCGN full length D161A/N163A	This study
hsSCGN D210A/S212A	GST-Tev-hsSCGN full length D210A/S212A	This study
hsSCGN D254A/N256A	GST-Tev-hsSCGN full length D254A/N256A	This study
hsSCGN	2xHA-hsSCGN full length	This study
hsSCGN_F225A	2xHA-hsSCGN_F225A	This study
hsSCGN_M229A	2xHA-hsSCGN_M225A	This study
Human SNAP-25		
SNAP-25	His-thrombin-SNAP-25A-full length	(Yang et al., 2015)
SN1	GST-thrombin-SNAP-25A (11-83)	This study
SN2	GST-thrombin-SNAP-25A (138-206)	This study
SNAP-25 A	GST-thrombin-SNAP-25A (138-160)	This study
SNAP-25 B	GST-thrombin-SNAP-25A (161-206)	This study
SNAP-25 C	GST-thrombin-SNAP-25A (138-180)	This study
SNAP-25 D	GST-thrombin-SNAP-25A (181-206)	This study
SNAP-25 E	GST-thrombin-SNAP-25A (161-180)	This study
SNAP-25 F	GST-thrombin-SNAP-25A (138-170)	This study
SNAP-25 G	GST-thrombin-SNAP-25A (148-180)	This study
SNAP-25 H	GST-thrombin-SNAP-25A (148-170)	This study
SNAP-25 I	GST-thrombin-SNAP-25A (138-165)	This study
SNAP-25 J	GST-thrombin-SNAP-25A (143-170)	This study
SNAP-25 J L160A	GST-thrombin-SNAP-25A (143-170) L160A	This study
SNAP-25 J A164S	GST-thrombin-SNAP-25A (143-170) A164S	This study
SNAP-25 J G155D	GST-thrombin-SNAP-25A (143-170) G155D	This study
SNAP-25 J G158S	GST-thrombin-SNAP-25A (143-170) G158S	This study
SNAP-25 J R161H	GST-thrombin-SNAP-25A (143-170) R161H	This study

SNAP-25 J R170H	GST-thrombin-SNAP-25A (143-170) R170H	This study
SNAP-25b	2xHA-SNAP-25b full length	This study
SNAP-25b_G155D	2xHA-SNAP-25b_G155D	This study
SNAP-25b_R161H	2xHA-SNAP-25b_R161H	This study
dmSNAP-25	MBP-fly-SNAP-25	This study
SNAP-23	GST-SNAP-23 ()	This study
SNAP-29	GST-SNAP-29 ()	This study
SNAP-47	GST-SNAP-47 ()	This study
OTHER		
Cbp53e	GST-TEV- fly SCGN full length	This study
synaptobrevin	GST-thrombin-rat synaptobrevin (29-94)	(Yang et al., 2015)
syntaxin 1A	GST-thrombin-rat syntaxin 1A (191-253)	(Yang et al., 2015)
SNAP-25 guideRNA	pLentiCRISPRv1-sgSNAP-25	This study
SCGN guideRNA	pLentiCRISPRv1-sgSCGN	This study

Table S3. Summary of Antibodies Used in this Study

Antibody	Source	Catalog#
SCGN	Santa Cruz	SC-374355
SNAP-25	Abcam	Ab5666
Syntaxin-1	Santa Cruz	SC-12736
HA	Biolegend	901502
β-Actin	Sigma	A5441
Alexa Fluor 488	Life Technologies	A11029
Alexa Fluor 555	Life Technologies	A21428

Table S4: Sequences of primers, CRISPR targeting regions, and Morpholino

sqRT-PCR primer	
Gapdh	CTGGTGACCCGTGCTGCTTT (forward)
	GTTTGCCGCCTTCTGCCTTA (reverse)
Huc	CTATGTGGATCCCAACGACGCCGAC (forward)
	CAACTGCTCCATGTCTTTCTG (reverse)
CRISPR target sequences (PAM)	
SCGN KO STC-1 cells	CCGCACGCAGAAAAACTCCAGCT (in exon 1)
SCGN KO STC-1 cells	CCGAGGCCGCATACTGATGAAAG (in exon 3)
SNAP-25 KO STC-1 cells	AGACATGCGCAATGAGCTGG (in exon 1)
SCGN KO zebrafish	CCAACCTAGATGCTGCCGGGTTT (in exon 1)
SCGN KO zebrafish	CTACATTGAAGGGAAAGAGCTGG (in exon 2)
Zebrafish Genotyping	
F1	CATTGAAGGGAAAGAGCT
F2	GTCTACATTGAAGGGACT
reverse	TGAGCATTTAAGAGAAACGACA
Morpholino	
scgn MO1	GGTTGGCAAAAGCACTGTCCATGAT
scgn MO2	GTGGTTTATGTTTGATACCTTTGGC
control	CCTCTTACCTCAGTTACAATTTATA
p53 MO	GCGCCATTGCTTTGCAAGAATTG